Resolution-independent diagnostics of solar magnetic fields

Jan Stenflo
ETH Zurich and
IRSOL, Locarno

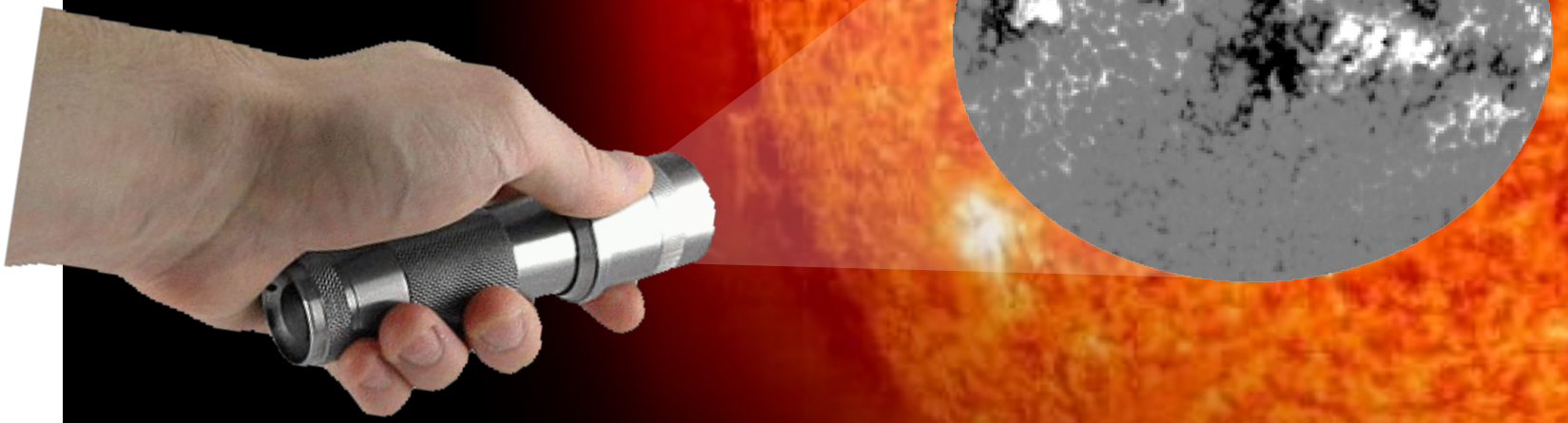

Fractal-like magnetic structuring on the quiet Sun

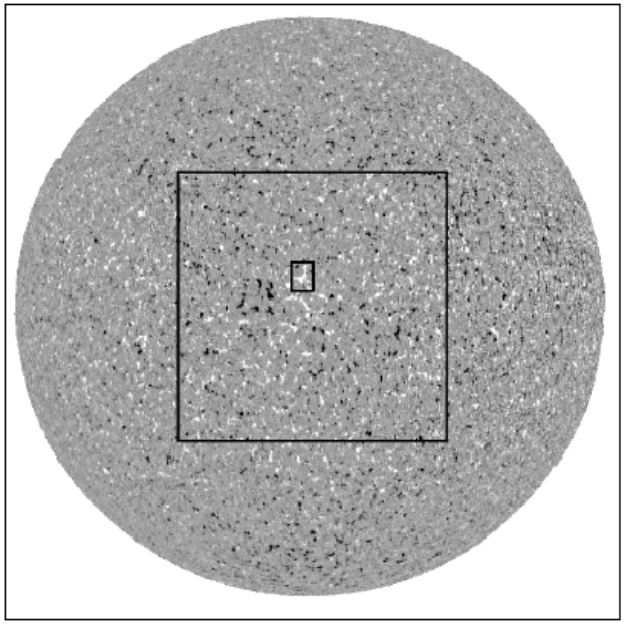

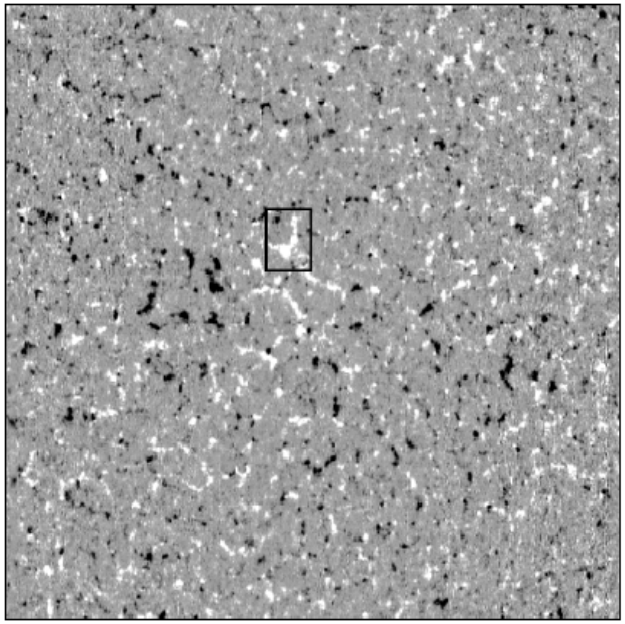

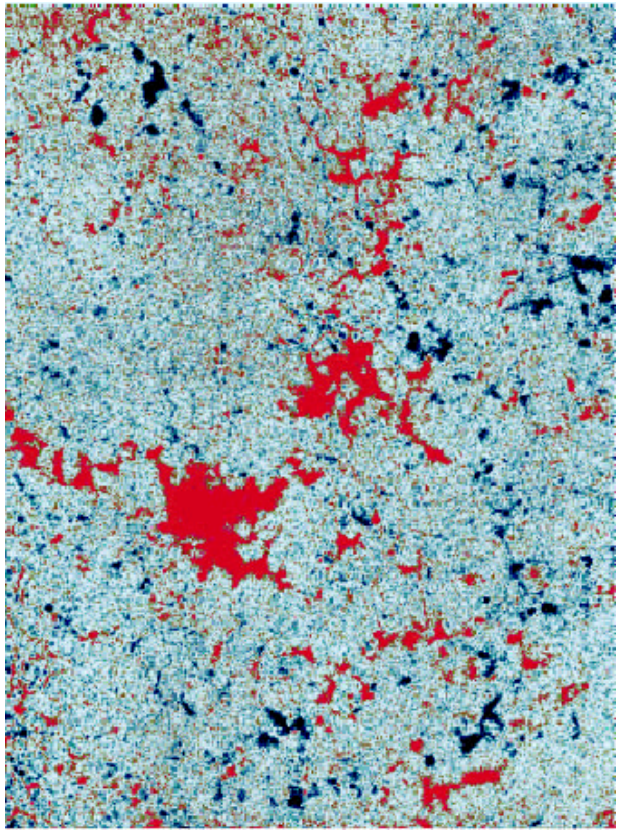

Institute of Astronomy ETH Zurich

IRSOL

Magnetic energy spectrum over 7 orders of magnitude in scale

25 m scale: the magnetic field ceases to be frozen-in and decouples from the plasma

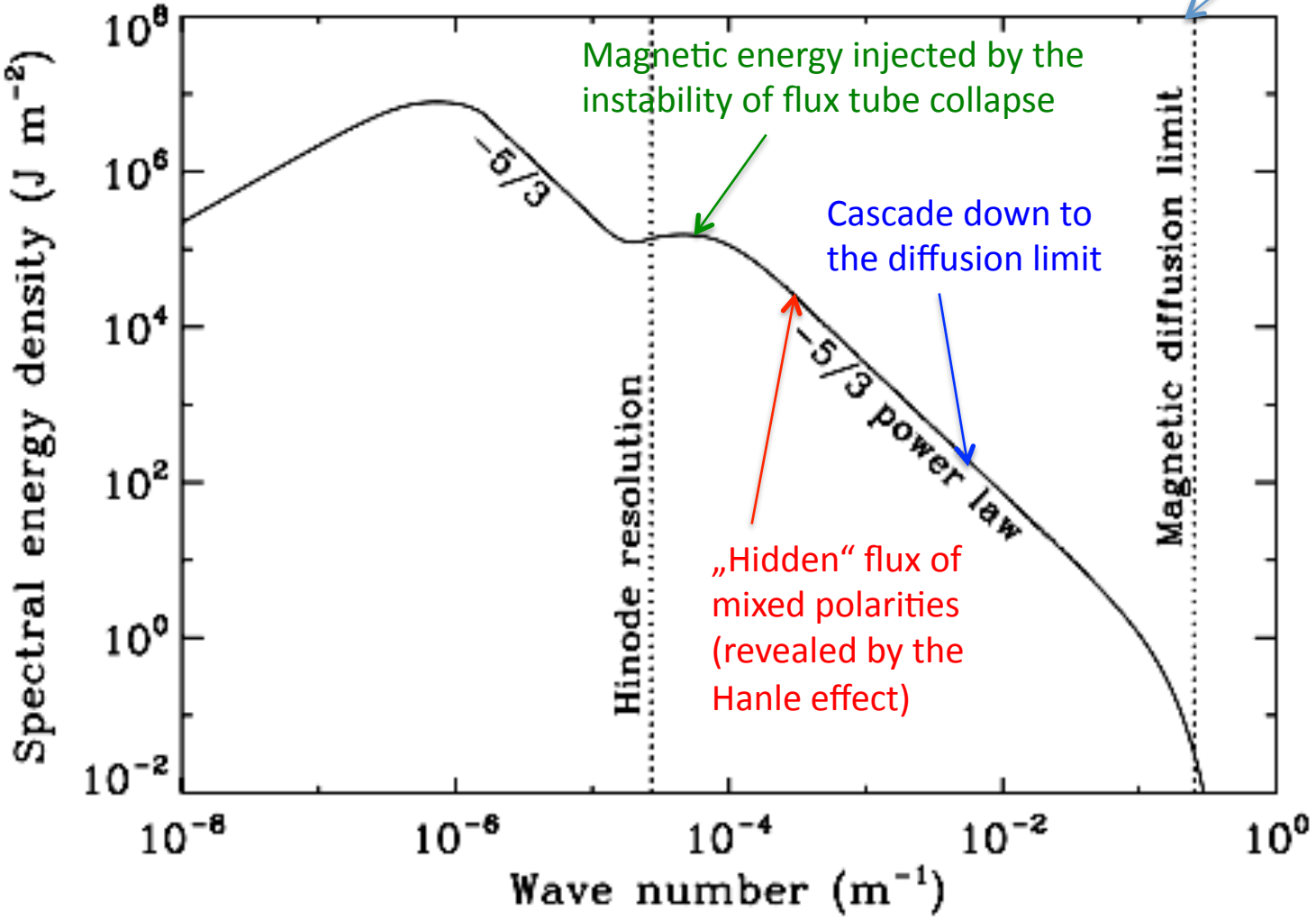

From
Stenflo, 2012,
A&A 541, A17

Institute of Astronomy
ETH Zurich

Resolution-independent magnetic-field diagnostics

Magnetic line-ratio technique (5250/5247), which allowed the discovery of **extreme intermittency**, with much of the photospheric magnetic flux is in the form of strong, **kG-type flux** bundles (flux tubes) with sizes nearly two orders of magnitude smaller than the spatial resolution at that time (Stenflo 1973).

Hanle depolarization technique, which led to the discovery that the photosphere is filled with an **ocean of hidden, turbulent fields** with mixed polarities on small scales (in the optically thin regime) and with strengths of order 10-100 G (Stenflo 1982).

Technique of using the **symmetry properties of the transverse Zeeman effect** for observations away from disk center (Stenflo 1987), to determine whether the **angular field distribution** favors the vertical or horizontal orientation (Stenflo 2013). The internetwork field is found to be preferentially vertical in the low to mid photosphere, but becomes preferentially horizontal in the upper photosphere.

Institute of Astronomy ETH Zurich

Hanle effect

Precessing classical oscillator

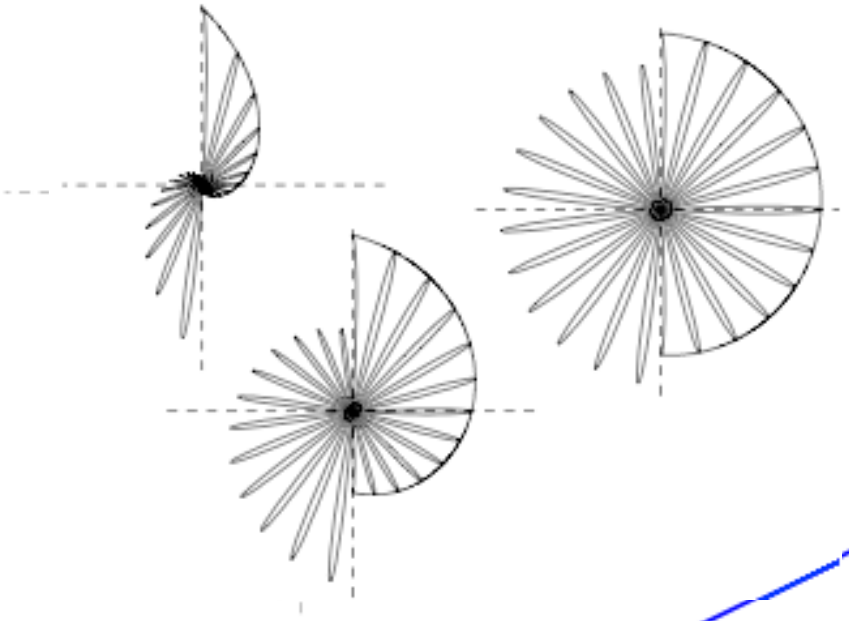

Ca I 4227 Å, a chromospheric line

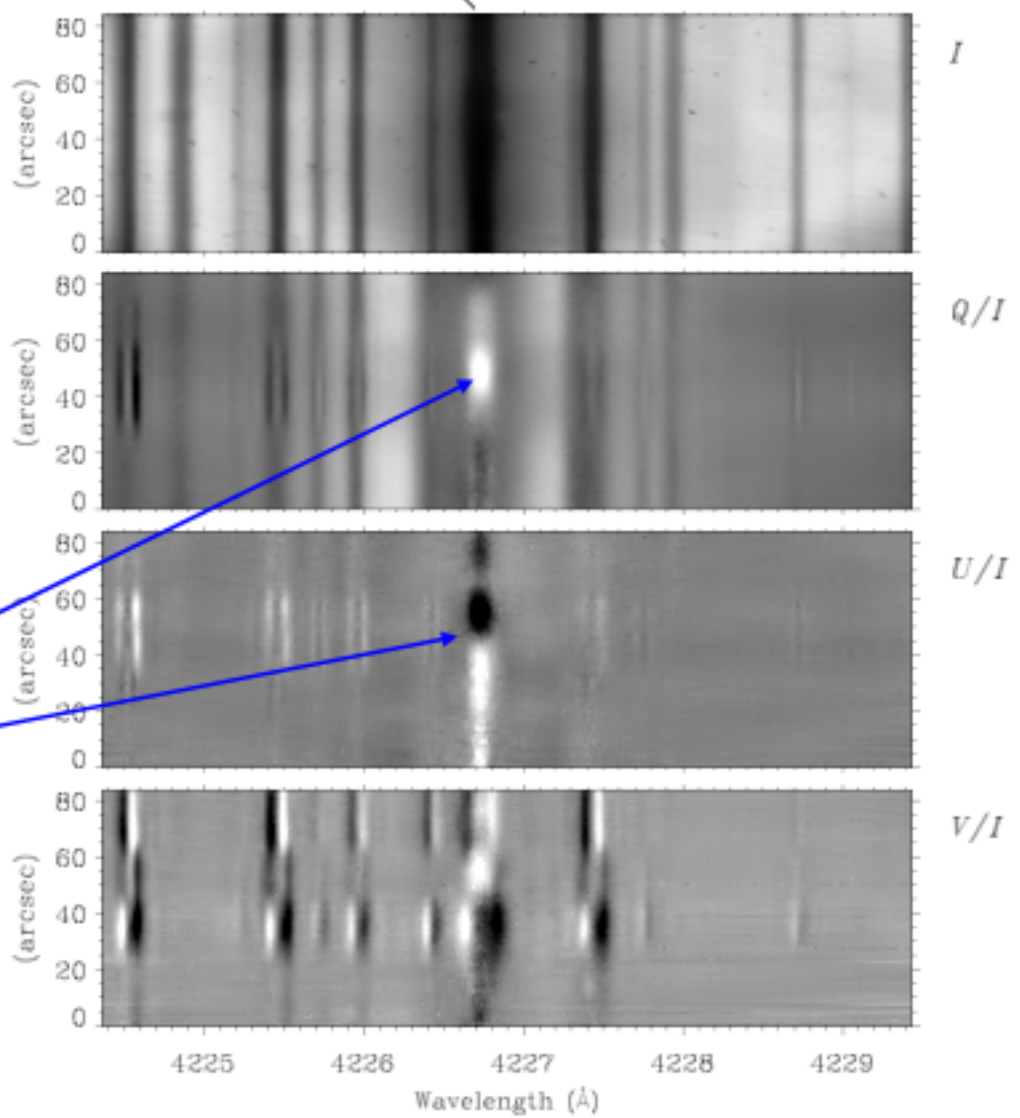

Hanle depolarization and rotation of the plane of polarization in the line core

Institute of Astronomy ETH Zurich

IRSOL

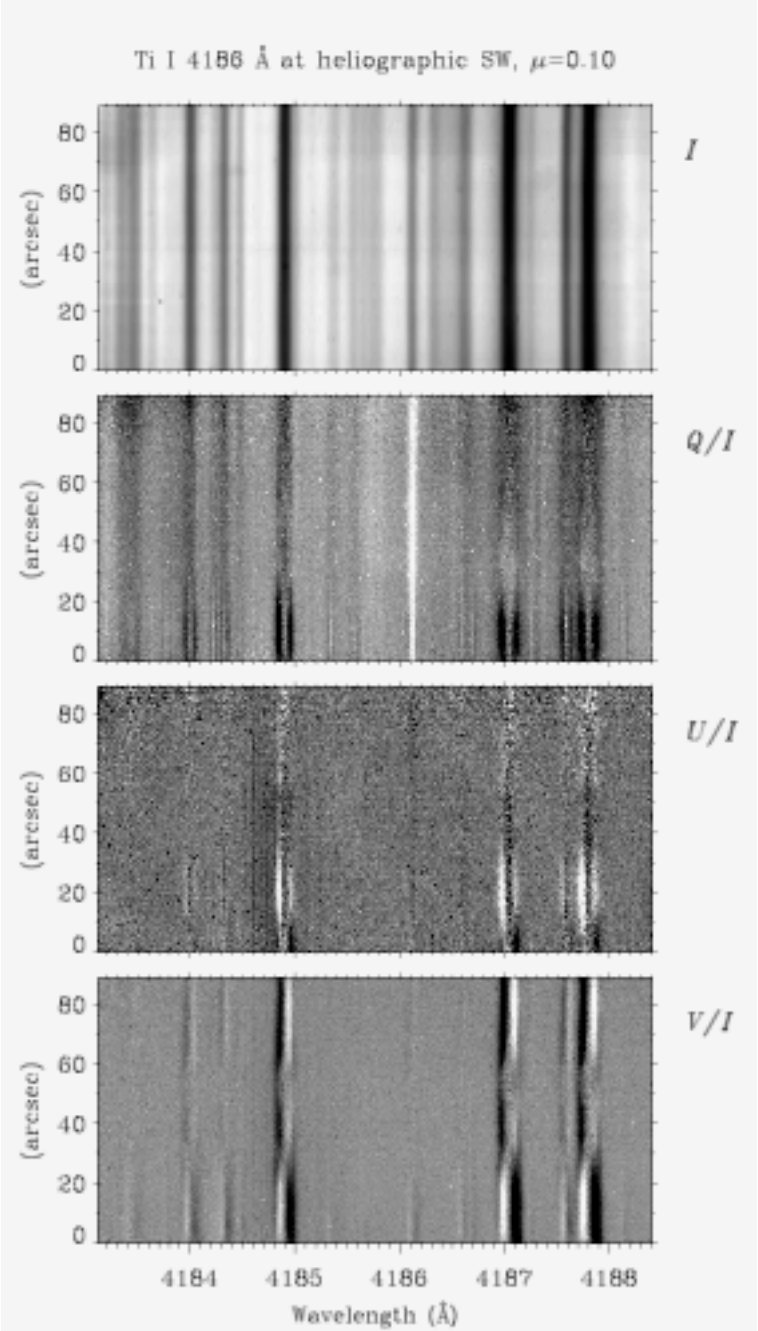

Difference between photospheric and chromospheric lines

In contrast to chromospheric lines, photospheric lines like the Ti I 4186 Å line (here shown to the left) or the often used Sr I 4607 Å line show no significant structuring along the slit (constant *Q/I*) and no significant rotation of the plane of polarization (zero (*U/I*).

At the same time the polarization amplitude in *Q/I* is much smaller than theoretically expected, which can only be explained in terms of Hanle depolarization caused by "hidden" magnetic fields.

In contrast, for chromospheric lines the observed fluctuations of *Q/I* and *U/I* are of similar magnitude, which is evidence that much of the magnetic fields that cause the observed Hanle signatures are spatially resolved.

Institute of Astronomy ETH Zurich

Signature of microturbulent magnetic fields

The only known explanation for the systematically reduced *Q/I* amplitudes of photospheric lines is Hanle depolarization caused by magnetic fields.

The absence of signatures in *U/I* shows that there is no net Hanle rotation of the plane of polarization. This can only be explained if the magnetic elements causing the Hanle depolarization in *Q/I* are much smaller than the spatial resolution and have mixed polarities, so that there is approximate balance between positive and negative Hanle rotations, leading to cancellation.

The absence of spatial structures in *Q/I* supports this interpretation.

Since the Hanle depolarization points to fields > 60 G (Trujillo Bueno et al. 2004) while the basal flux density at the Hinode scale is only 3.5 G (Stenflo 2012), the „hidden“ flux elements must be much smaller than the Hinode scale (230 km).

As the transition between the optically thick and thin regimes is around the 100 km scale, the bulk of the turbulent elements must be optically thin, which means that we have **microturbulence**.

Institute of Astronomy ETH Zurich

The inferred hidden flux from the observed Hanle depolarization, with B > 60 G,
is too large to be accounted for by a Kolmogorov -5/3 power law in the inertial range.
If it is raised to a -1.0 power law instead, we restore consistency with the Hanle results.
The extra mechanism to create this much flux may come from a local dynamo.
It can be shown that the local dynamo does not play any significant role at resolved scales
(Stenflo 2012).

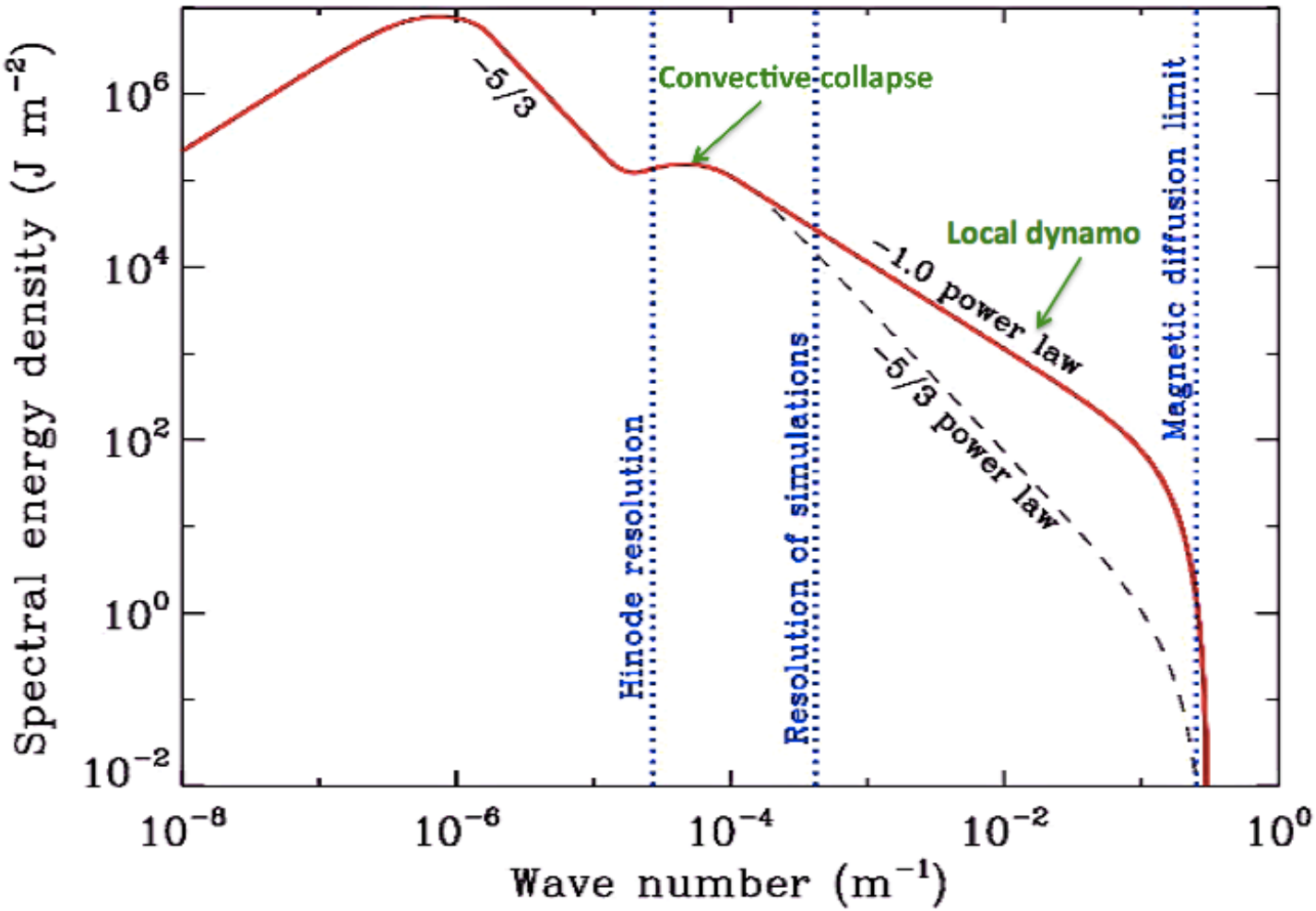

Institute of Astronomy ETH Zurich

IRSOL

Effect of power-law index on the rms field strength

The magnetic energy spectrum has been integrated from the small-scale end (the diffusion limit) to give the cumulative energy up to a given scale size. Taking the square root and converting to G units gives the rms field strength. Best consistency with the Hanle constraints is obtained for power-law index -1.0.

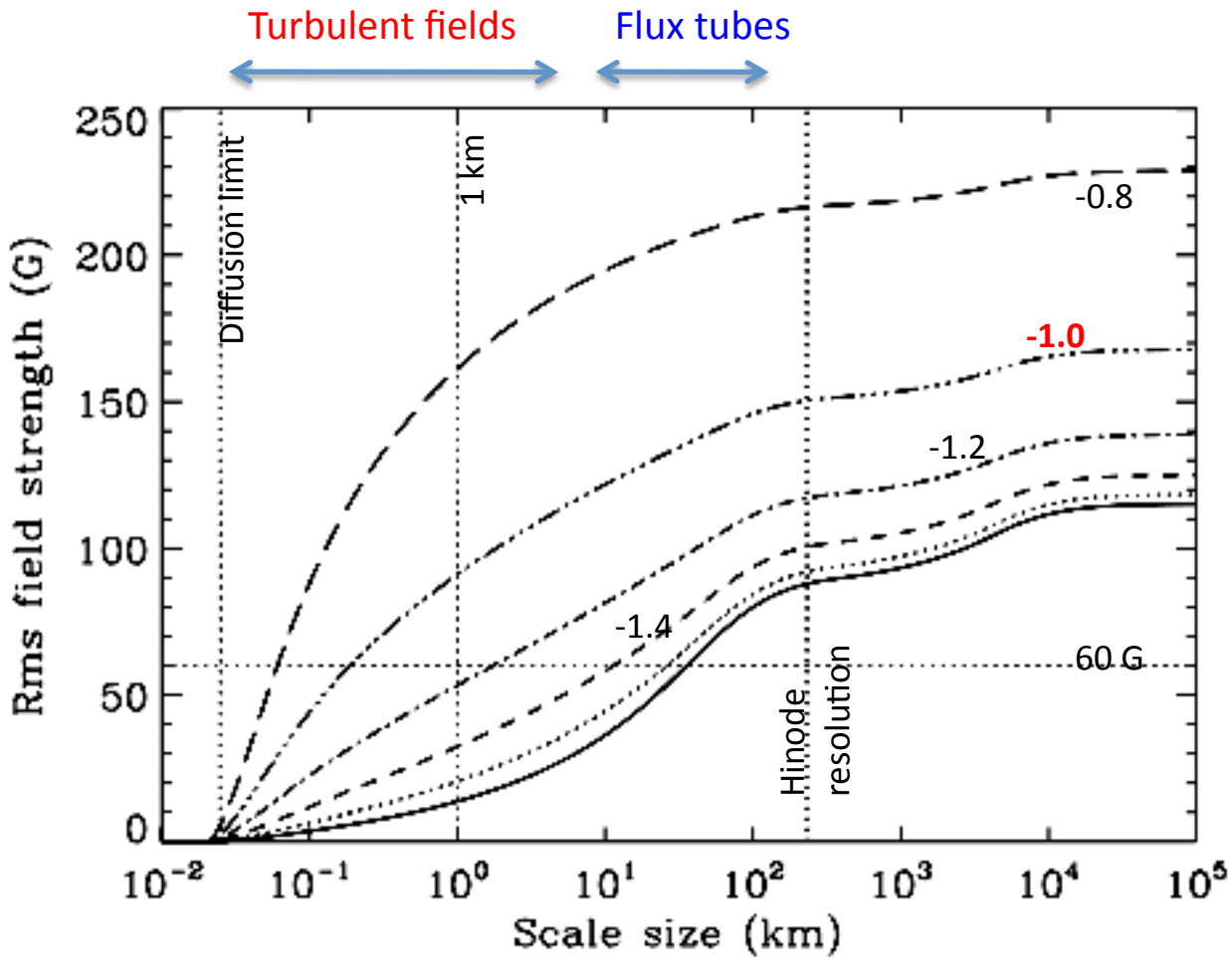

Institute of Astronomy ETH Zurich

The Sun‘s basal flux level (in the absence of sunspots) is very low

2002

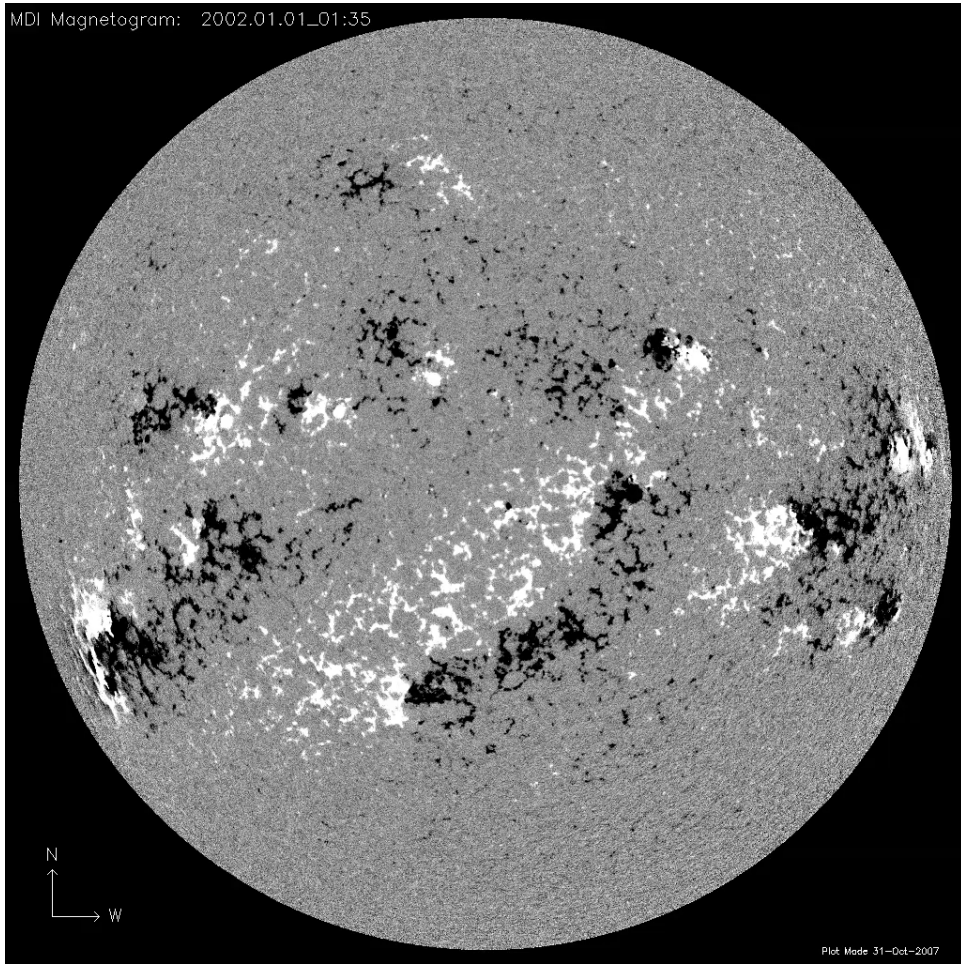

2009

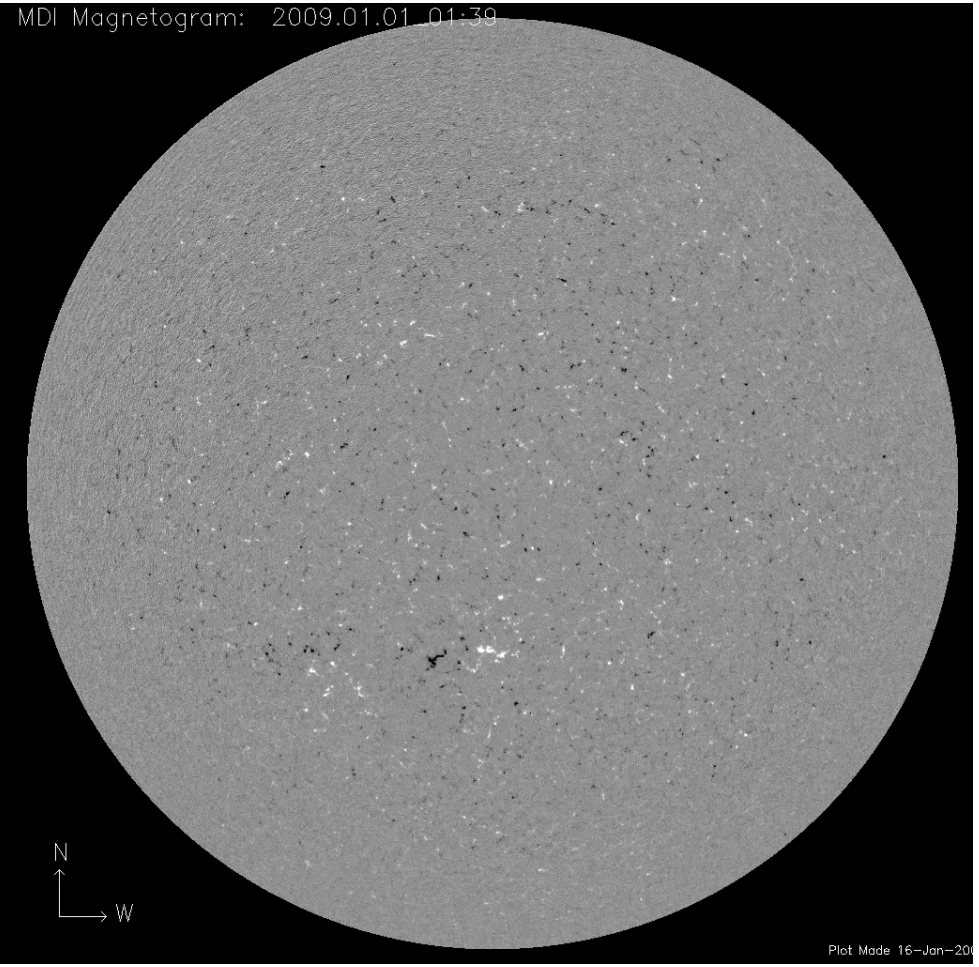

Institute of Astronomy ETH Zurich

IRSOL

Cycle variation of the unsigned flux density after noise removal

Solid curve: Monthly average of the unsigned vertical flux density $|B_v|$, averaged over a circular region around disk center with radius r (in units of the radius of the solar disk) < 0.9, after the noise contribution has been removed.

The dashed curve is the second-order fit function in terms of the sunspot number R_z, $b_0 + b_1 R_z + b_2 R_z^2$, where b_0 represents the average unsigned flux density in the absence of sunspots.

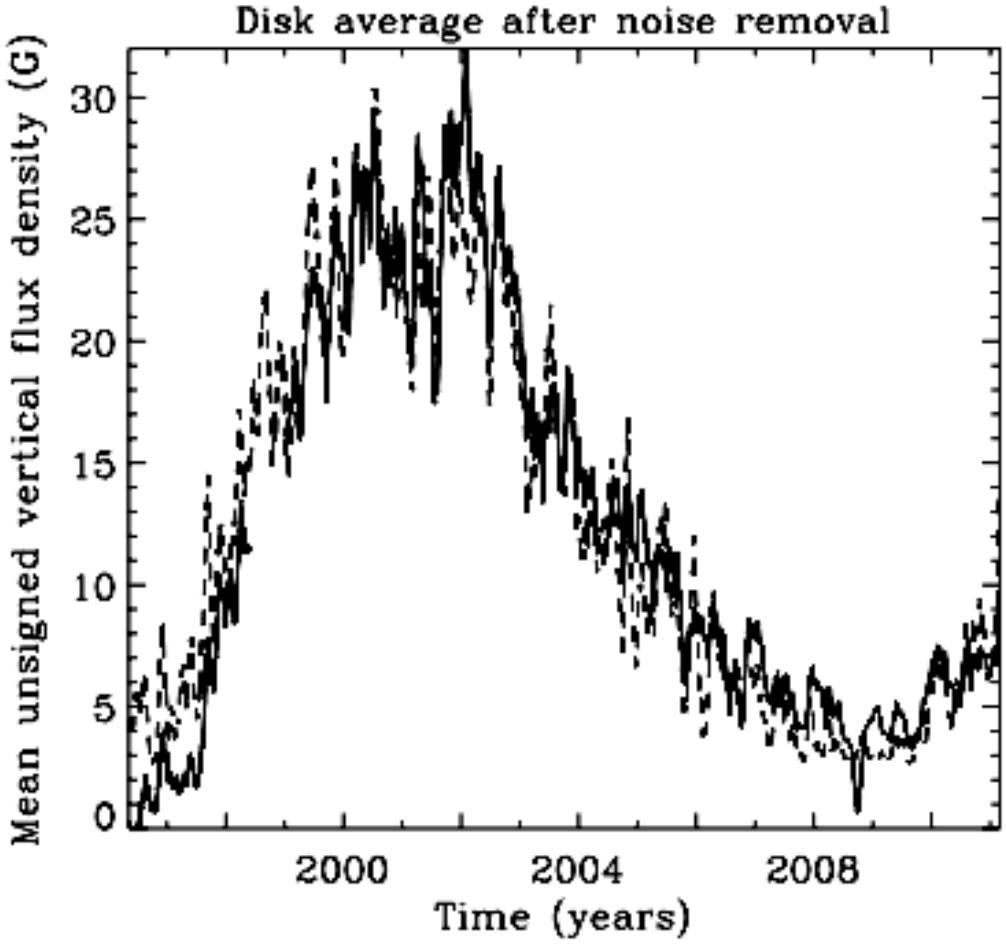

Coefficient b_0, which represents the basal flux density in the absence of sunspots, is **2.7 G**.

At activity maximum there is 10 times more flux on the Sun than the basal level

Institute of Astronomy ETH Zurich

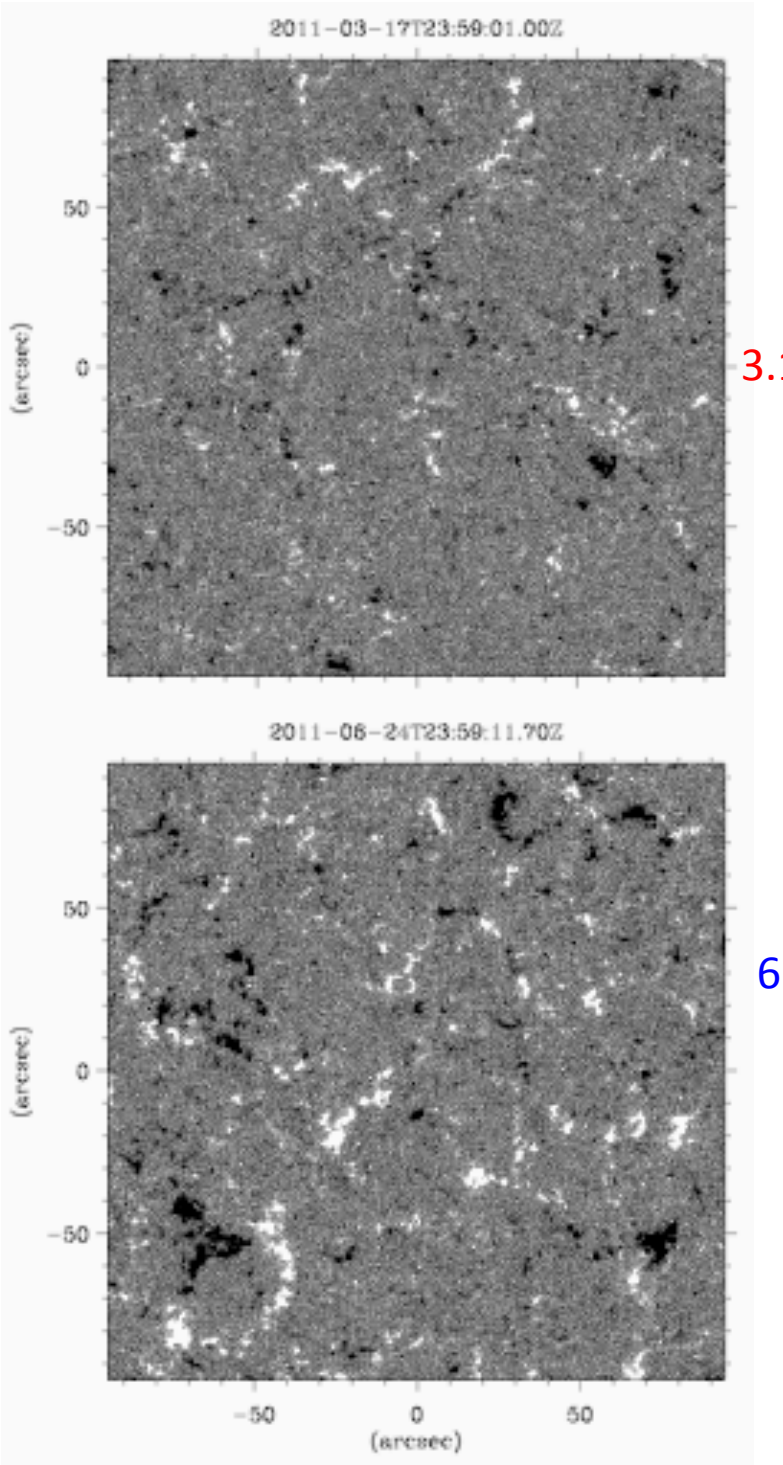

3.1 G

6.7 G

Examples of two HMI magnetograms
for $| r | < \pm 0.1\, r_{\odot}$

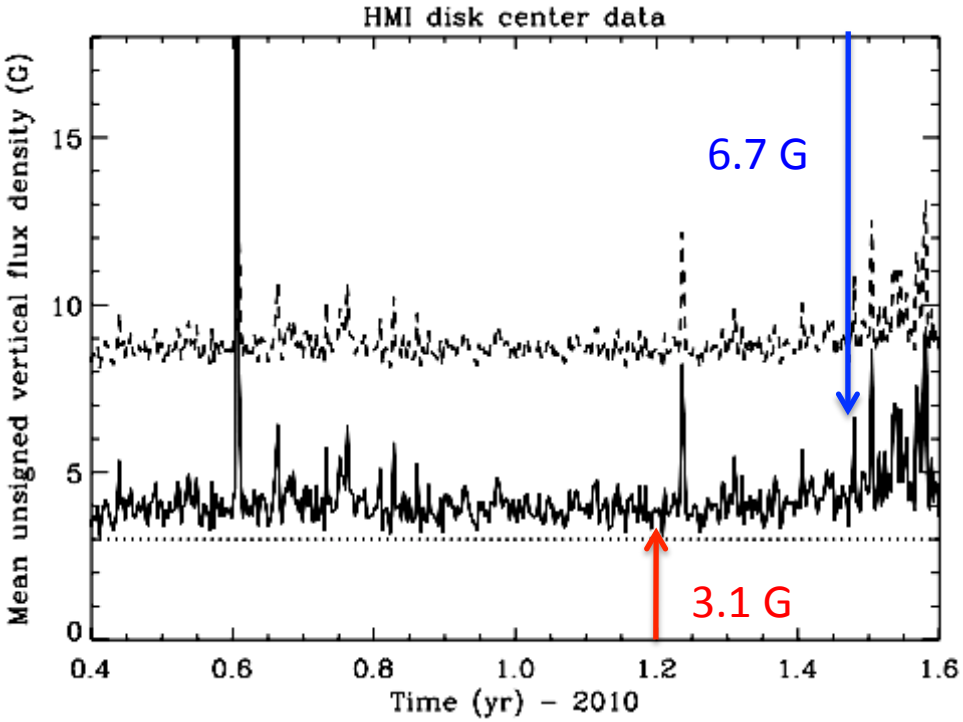

Both magnetograms represent the quiet Sun, but the amount of flux differs by more than a factor of two. Any such variations have their source in the global dynamo.

Institute of Astronomy ETH Zurich

IRSOL

Quiet-sun PDFs with Gaussian noise core

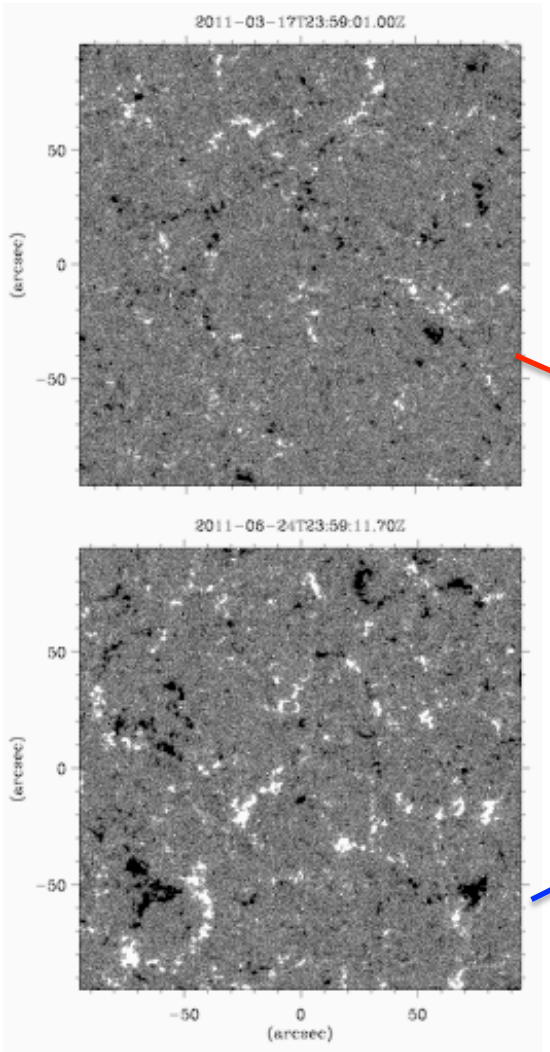

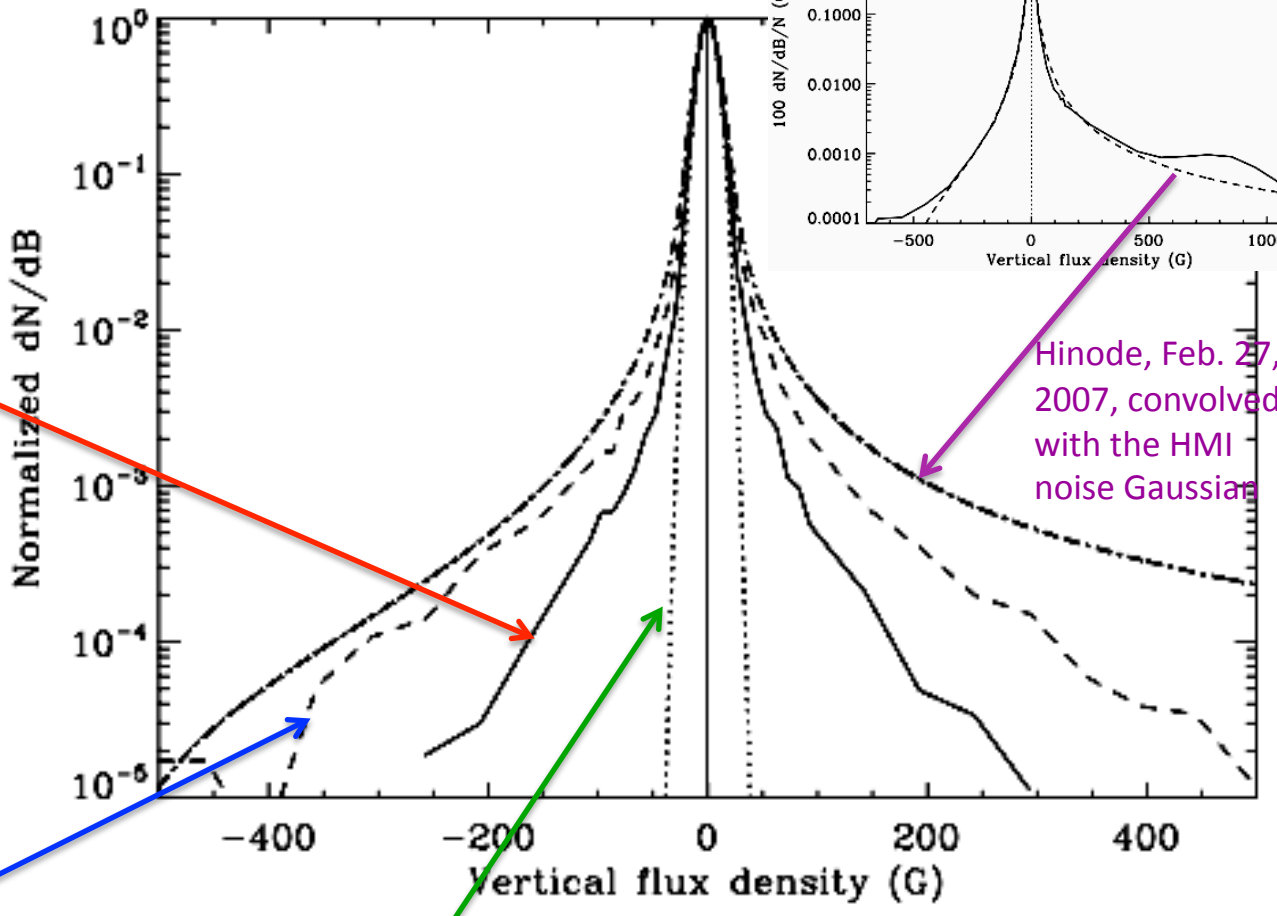

Hinode, Feb. 27, 2007, convolved with the HMI noise Gaussian

HMI noise

The intrinsic (noise-free) PDF core is extremely narrow. The dominating contribution to the intrinsic flux comes from the PDF „damping wings“, which represent intermittent flux.

Institute of Astronomy ETH Zurich

Horizontal or vertical magnetic fields

Angular distribution of the field vectors
determined from the symmetry properties of the transverse Zeeman effect
when observed away from disk center.

The determination whether the field is more vertical or more horizontal
then becomes, in a statistical sense, both model and resolution independent.

Symmetry of Stokes *Q* or *U* :

(sign pattern -+- or +-+)

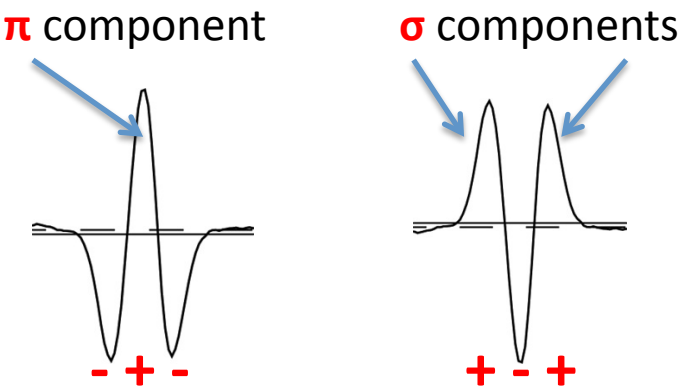

Symmetry of Stokes *V* :

(sign pattern +- or -+)

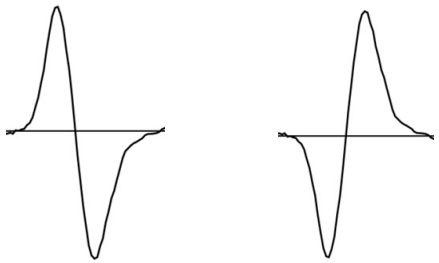

Institute of Astronomy ETH Zurich

Let us define the Stokes coordinate system for observations away from disk center such that the **positive Stokes *Q* direction is perpendicular to the radius vector** (parallel to the nearest solar limb. Then, if for observations near the limb the transverse field component is along the radius vector, i.e., predominantly vertical, then (for absorption lines) the transverse Zeeman effect will give the Stokes *Q* pattern **- + -** . If the transverse field is perpendicular to the radius vector (predominantly horizontal), the pattern will be **+ - +** .

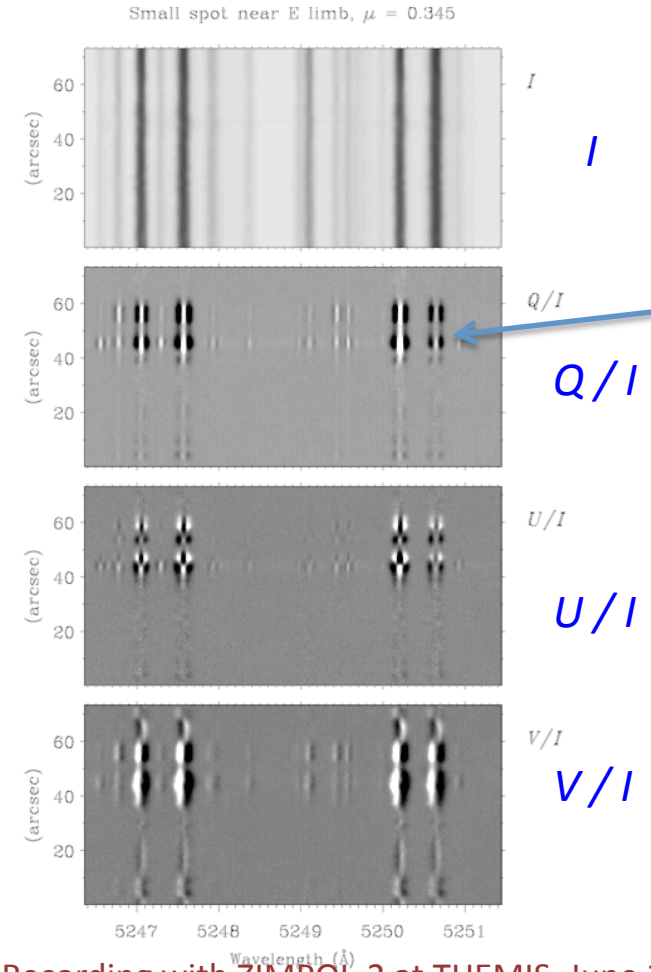

I

Q / I

U / I

V / I

Recording with ZIMPOL-2 at THEMIS, June 2008

Predominantly vertical fields:

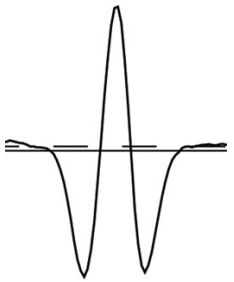

Predominantly horizontal fields:

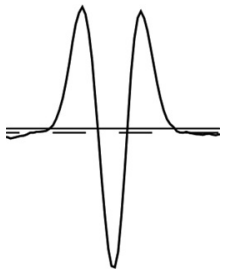

Institute of Astronomy ETH Zurich

IRSOL

We may write

$$Q = q_\lambda \, g_Q$$

$$U = u_\lambda \, g_U$$

$$V = v_\lambda \, g_V$$

where q_λ and u_λ are profile factors of the type 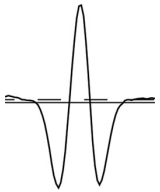

v_λ of the type 

g_Q , g_U and g_V are the angular factors

$$g_Q = \sin^2\gamma \cos 2\chi$$

$$g_U = \sin^2\gamma \sin 2\chi$$

$$g_V = \cos\gamma \, ,$$

where **γ** is the inclination, **χ** the azimuth **with respect to the line-of-sight**

Institute of
Astronomy
ETH Zurich

Transformation of the angles to a reference systems with respect to the vertical direction:

θ_B and ϕ are inclination and azimuth **with respect to the vertical of the atmosphere.**

$\mu_B = \cos\theta_B$, while μ is the cosine of the heliocentric angle.

$$g_Q = -\sin^2\theta_B \sin^2\phi + (\sin\theta \cos\theta_B - \mu \sin\theta_B \cos\phi)^2 ,$$

$$g_U = 2 \sin\theta_B \sin\phi \, (\sin\theta \cos\theta_B - \mu \sin\theta_B \cos\phi) ,$$

$$g_V = \mu \cos\theta_B + \sin\theta \sin\theta_B \cos\phi ,$$

Next we consider an ensemble of magnetic field elements with a directional distribution that is random in azimuth ϕ , while the distribution f_a of inclination angles θ_B is governed by the parameter a through

$$f_a \sim \mu_B{}^a .$$

Regimes:

$a = 0$: Isotropic distribution

$-1 < a < 0$: Pancake-like distribution (preference for horizontal fields)

$a > 0$: Peaked around the vertical direction (preference for vertical fields)

Institute of Astronomy ETH Zurich

Monte Carlo samplings of this angular distribution, illustrated for the case α = 1.5 (preferentially vertical)

Histograms of g_Q (solid), g_U (dashed), and g_V (dotted) for μ = 0.3

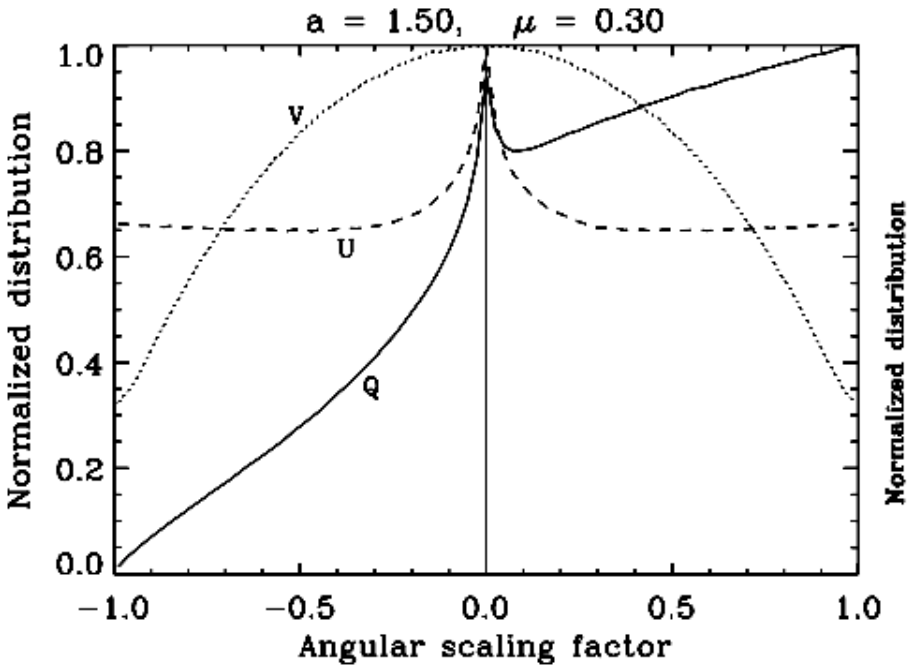

g_U and g_V are symmetric, only g_Q is asymmetric.

The ensemble average of g_Q is therefore non-zero

CLV of the g_Q histograms, from μ =1 (disk center) to μ = 0 (limb)

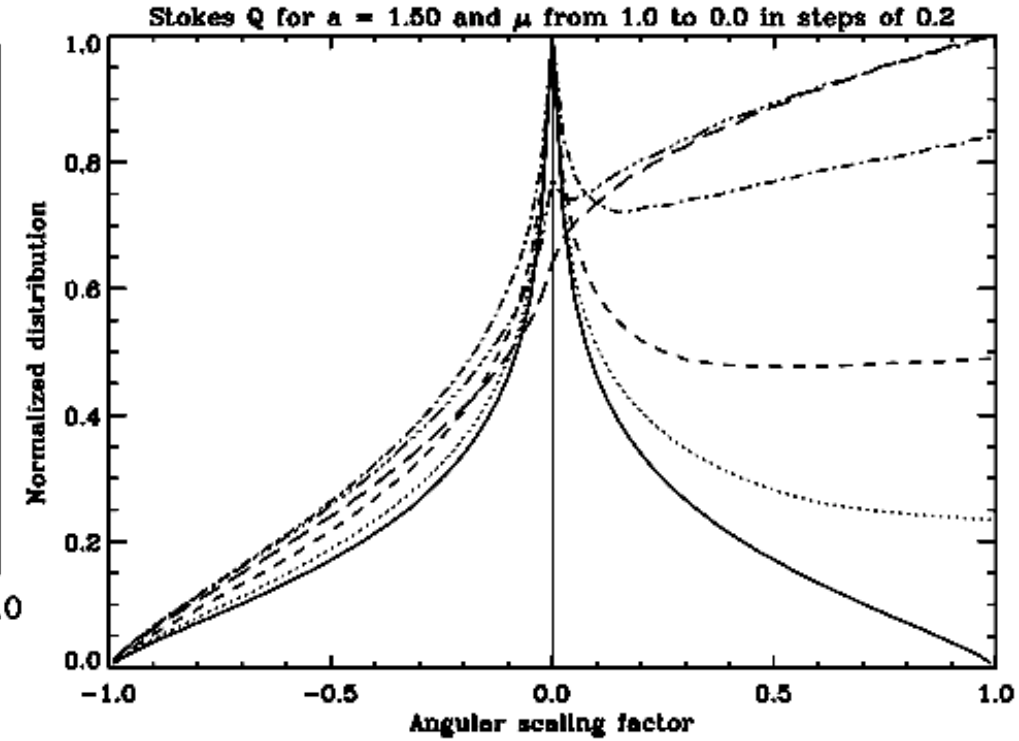

g_Q is symmetric at disk center but becomes increasingly asymmetric towards the limb

Institute of Astronomy ETH Zurich

Ensemble average of g_Q :

$$\bar{g}_Q = \frac{a}{a+3}(1-\mu^2)$$

where

$$1-\mu^2 = (r/r_\odot)^2$$

The sign of the ensemble average is given by the sign of parameter *a* and determines if the profile pattern is **- + -** or **+ - +** .

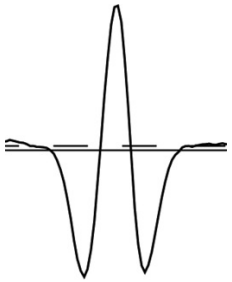

With this pattern the distribution deviates from the isotropic case ($a = 0$) in favor of vertical fields ($a > 0$)

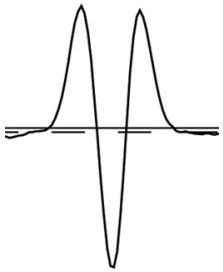

This pattern, for $a < 0$, reveals preference for horizontal fields

Institute of Astronomy ETH Zurich

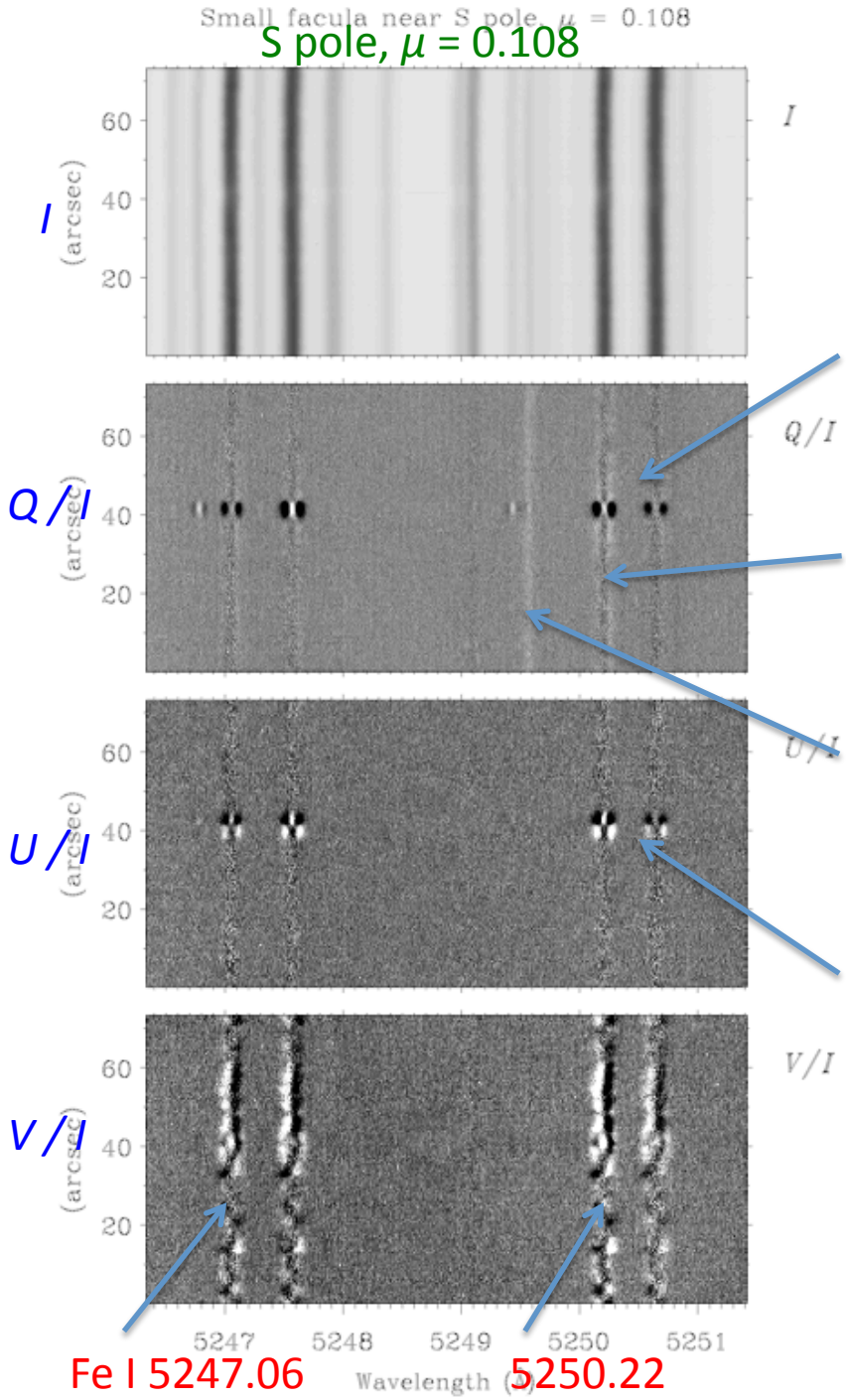

All the recordings were made with ZIMPOL-2 at the French THEMIS telescope on Tenerife, June 9-10, 2008

Small polar facula, sign pattern corresponds to vertical field

Weak background field with opposite sign pattern, implying preference for horizontal fields

Scattering polarization in Nd II (ionized neodynium)

Sign change in *U / I* (symmetry between + and -)

Institute of Astronomy ETH Zurich

IRSOL

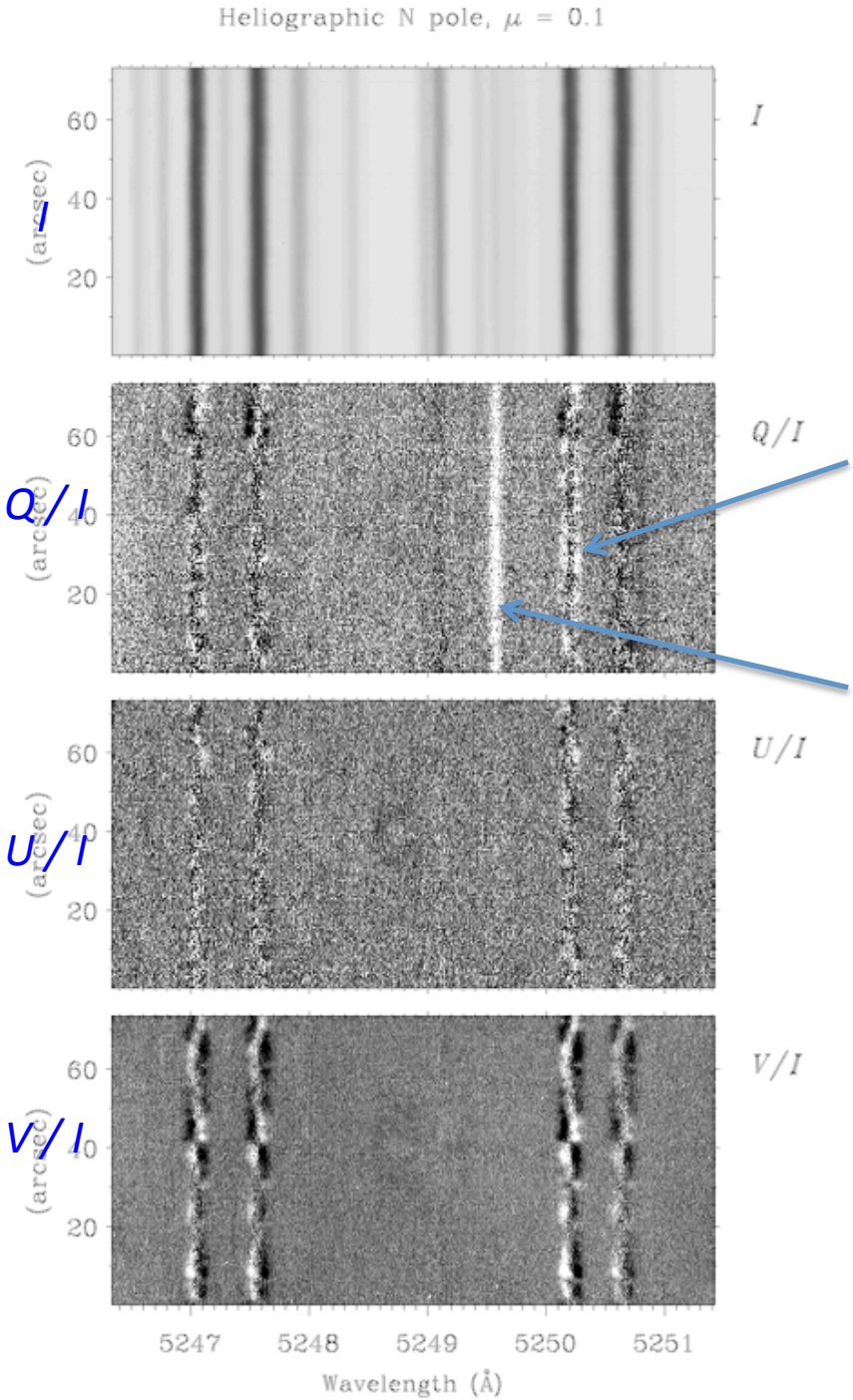

N pole, μ = 0.1 (5 arcsec inside limb)
Intranetwork fields (no polar faculae around)

Sign pattern indicates on average
preference for horizontal fields

Scattering polarization from neodynium

Institute of
Astronomy
ETH Zurich

Small spots near E limb

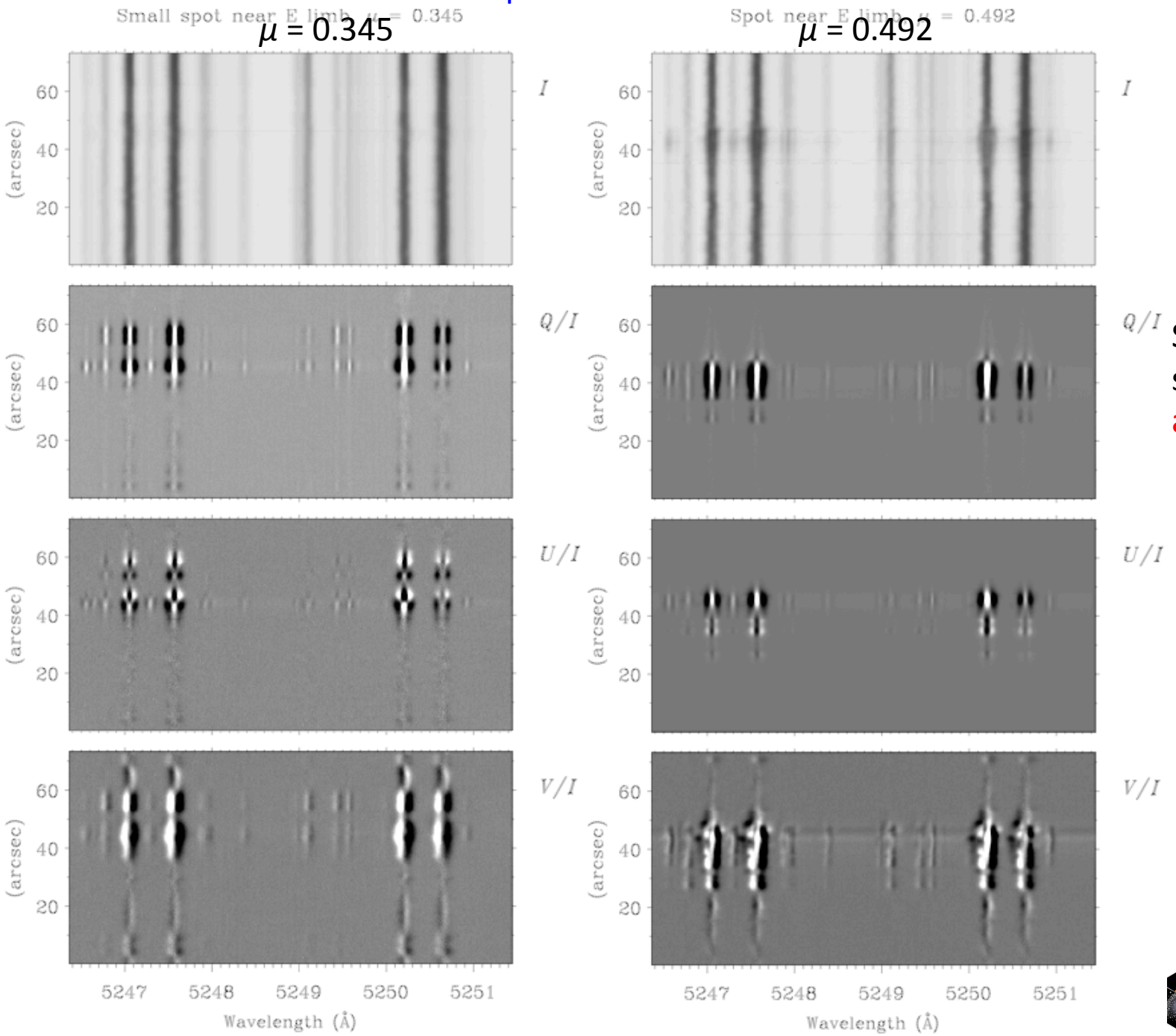

Sign pattern shows that fields are vertical

Institute of Astronomy ETH Zurich

IRSOL

Another spot near E limb

$\mu = 0.544$

Polar faculae near N pole

$\mu = 0.261$

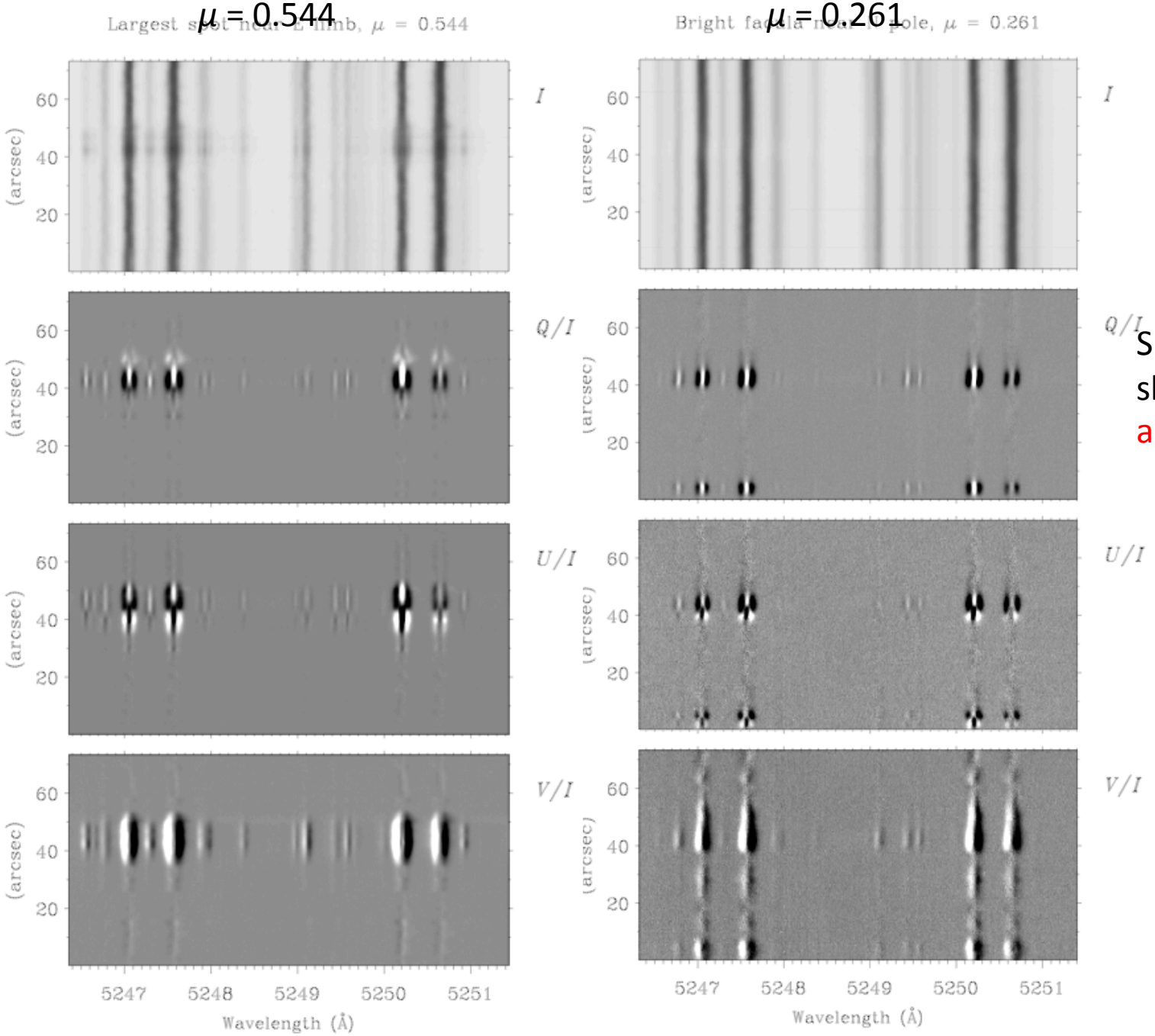

Sign pattern again shows that fields are vertical

Institute of Astronomy ETH Zurich

IRSOL

Faculae near E limb

$\mu = 0.413$ $\mu = 0.299$

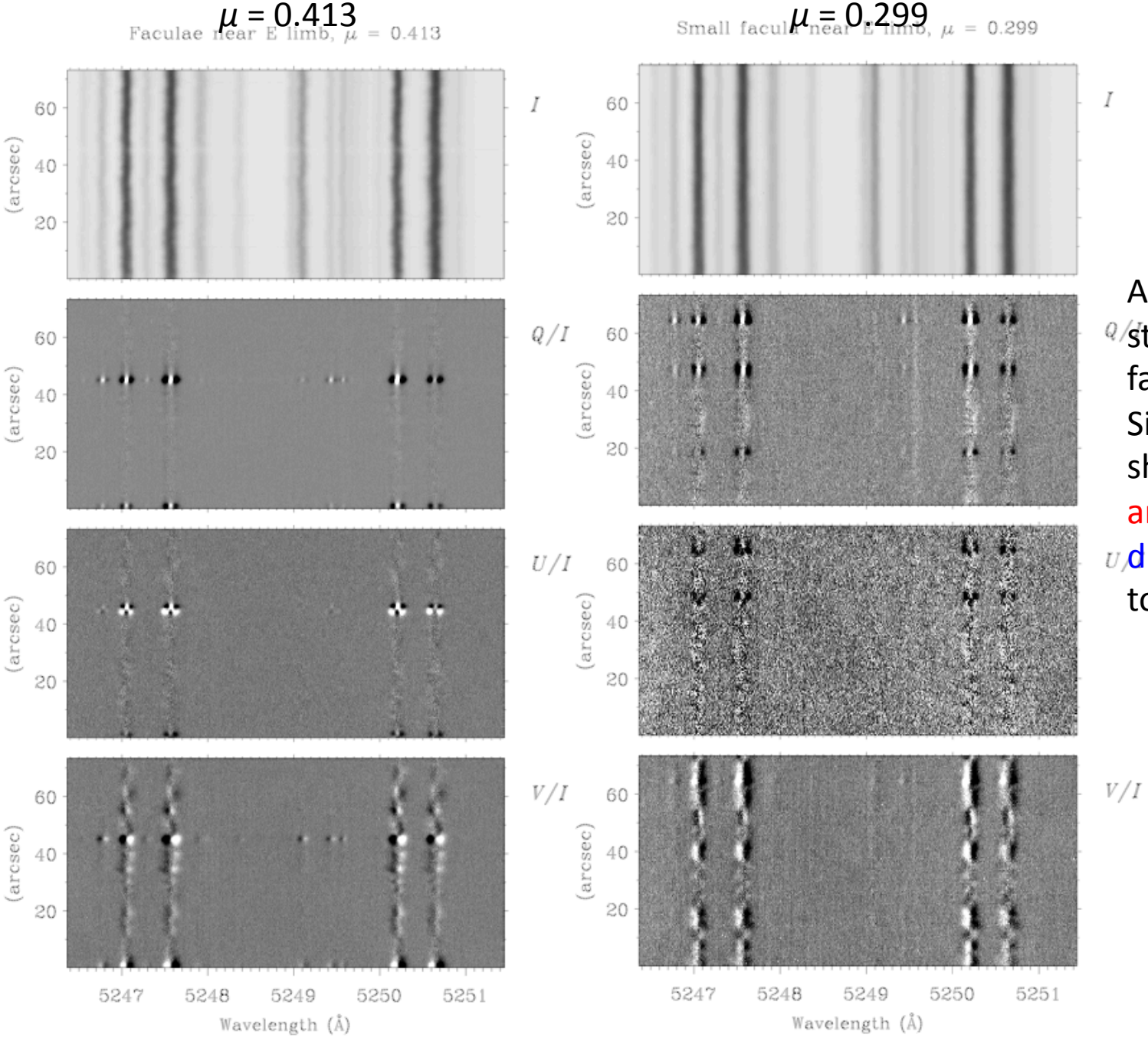

Always the same story for spots, faculae, and network: Sign patterns show that the fields are vertical for all limb distances, all the way to the extreme limb

Institute of Astronomy ETH Zurich

IRSOL

Previously shown recordings, both for $\mu = 0.1$ (5 arcsec inside the limb),
left for polar facula near S pole, right for intranetwork fields near N pole

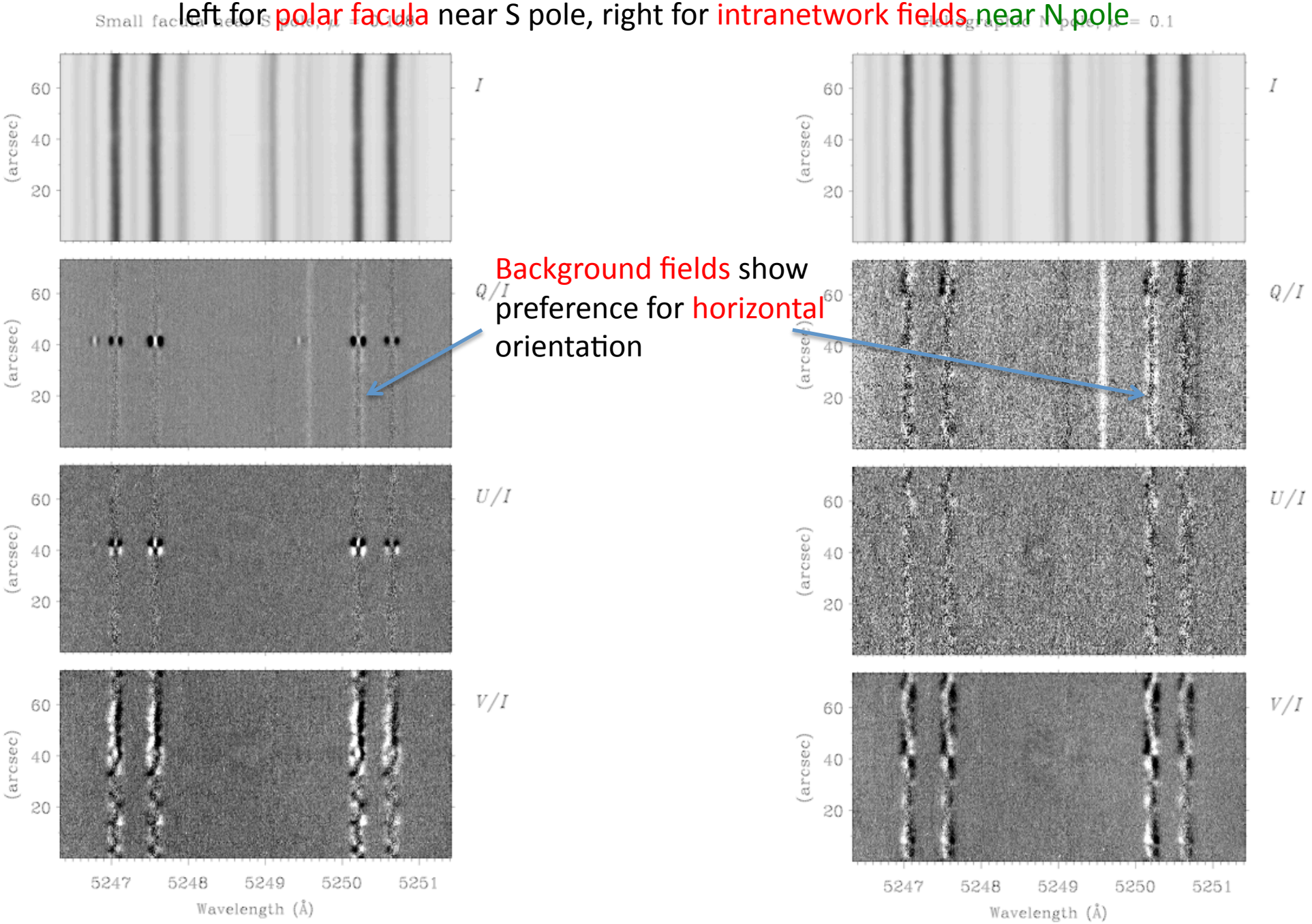

Background fields show preference for horizontal orientation

The same story for other intranetwork regions, here for two such regions near the E limb.
This indicates that the sampled behavior is statistically representative.

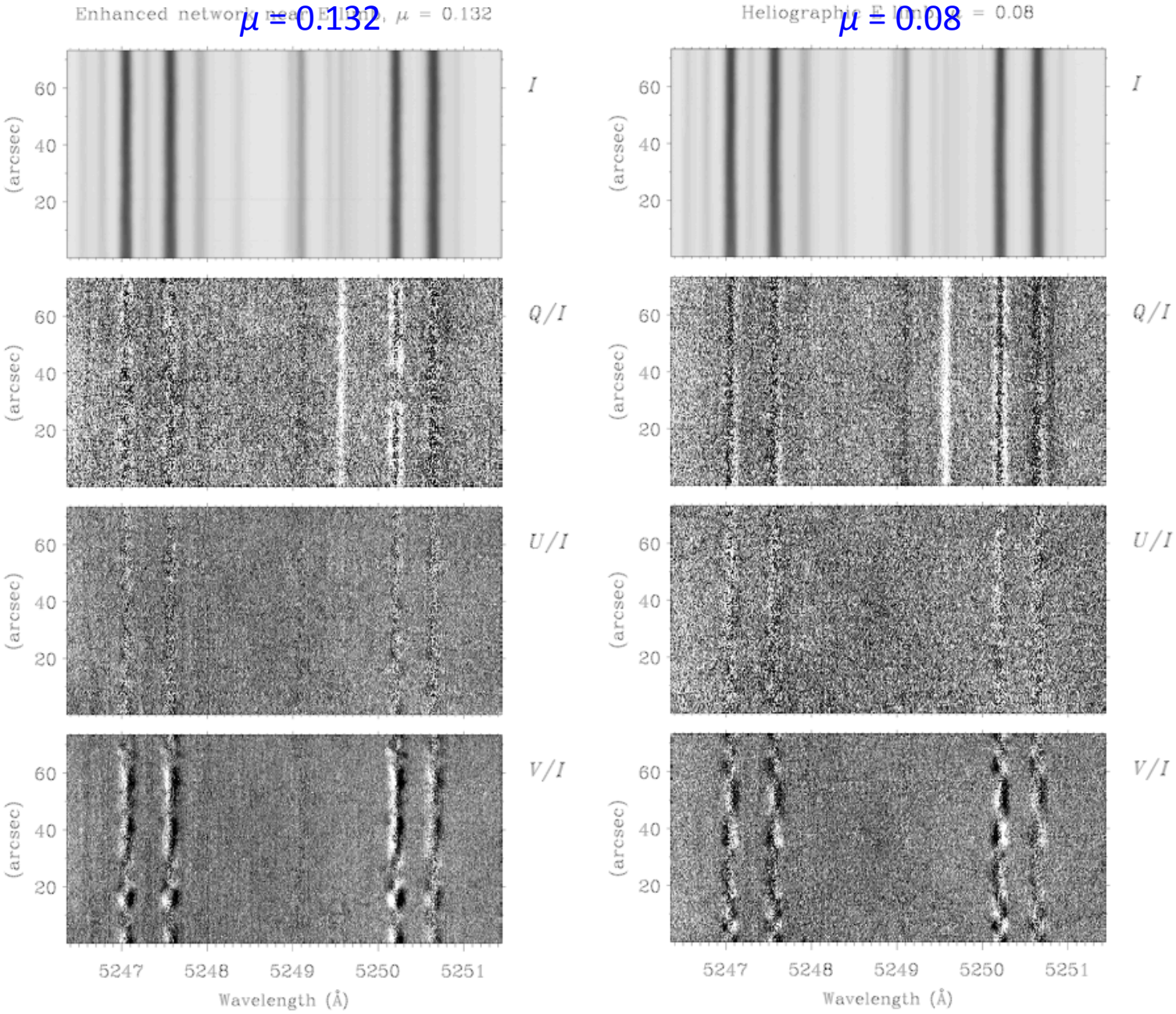

Institute of Astronomy ETH Zurich

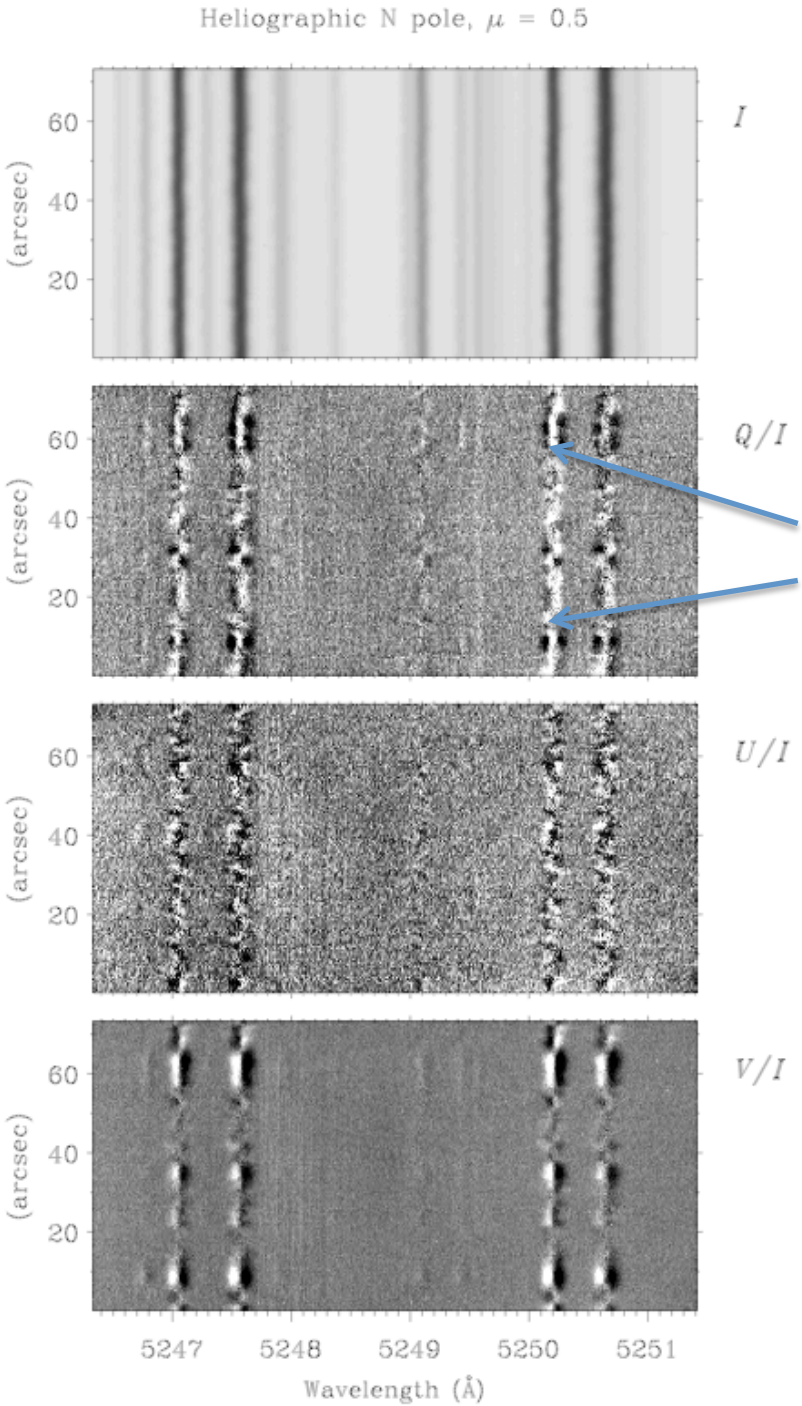

However, when we move away from the limb, the sign pattern of the intranetwork fields changes in favor of vertical orientation.

In the illustrated example, we have moved from the N pole along the central meridian to μ = 0.5

Now the π component is predominantly positive

In *U / I* the sign pattern has no particular preference. The profile shapes are anomalous, indicating the presence of unresolved magnetic elements with differing Doppler shifts.

Institute of Astronomy ETH Zurich

Center-to-limb variation of the ensemble averages of Q / I
for **7 intranetwork regions**
showing a **sign change at μ = 0.22** (zero-crossing of straight-line fit)

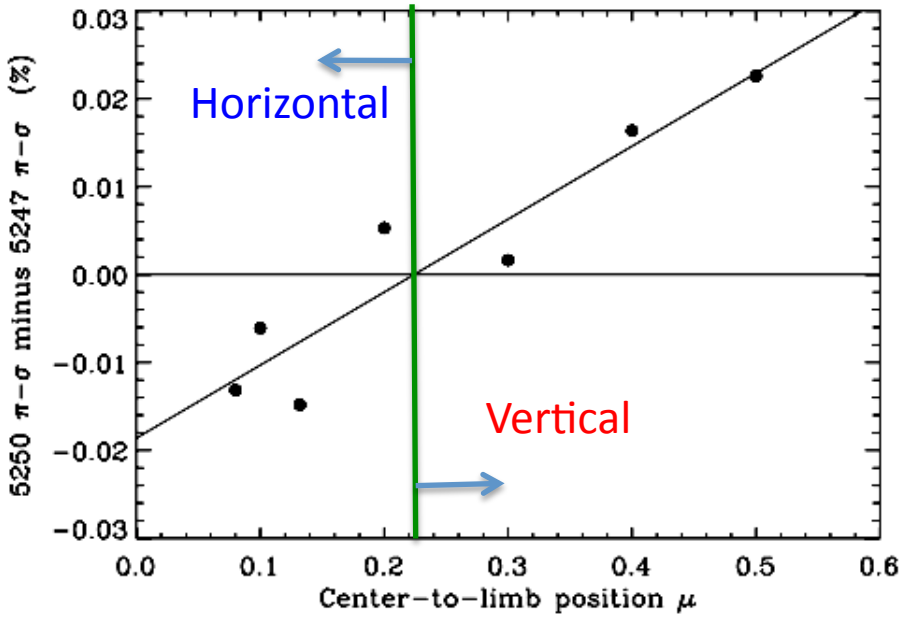

1-σ scatter of the points around the straight-line fit: 5 x 10^{-5}

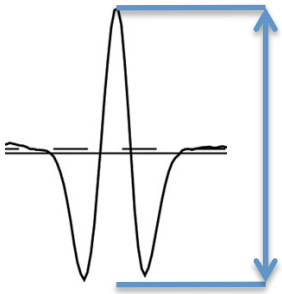

To suppress errors from drifts of the zero reference level and subtle polarized fringes we have applied a doubly differential technique:
The ensemble average is calculated for the difference between the amplitudes of the π components and the average of the two σ components, for each of the 5250.22 and 5247.06 Å lines.
Then we use the difference between the averages for the two lines.
Note that the linear polarization in the 5250.22 line is larger than that of the 5247.06 line by the factor 2.25 (squared Landé factor ratio.

Institute of Astronomy ETH Zurich

Height variation of the vertical-horizontal preference

Since the height of line formation increases with decreasing μ, our results describe the height variation of the horizontal-vertical preference.

Concentrated fields, like spots, faculae, and network, retain a vertical preference over the entire height range.

The weaker background (intranetwork) fields are more vertical in the lower-to-middle photosphere, but more horizontal in the upper photosphere (transition at $\mu \approx 0.2$)

The results are **model independent** in the sense of only making use of the fundamental symmetry property of the transverse Zeeman effect (the sign pattern).

The **results are independent of telescope resolution**, since they are only based on ensemble averages. Reason: Averaging over a given surface area of the Sun optically (because it is not resolved by the telescope used) or numerically over the resolved sub-areas give identical results.

Institute of
Astronomy
ETH Zurich

Factors competing to make the field more vertical or more horizontal:

- flux tube collapse due to superadiabatic stratifiction
- buoyancy forces pushing the anchored fields in the vertical direction
- expansion with height due to the pressure drop with height
- field topology: only fields with widely separated footpoints reach high

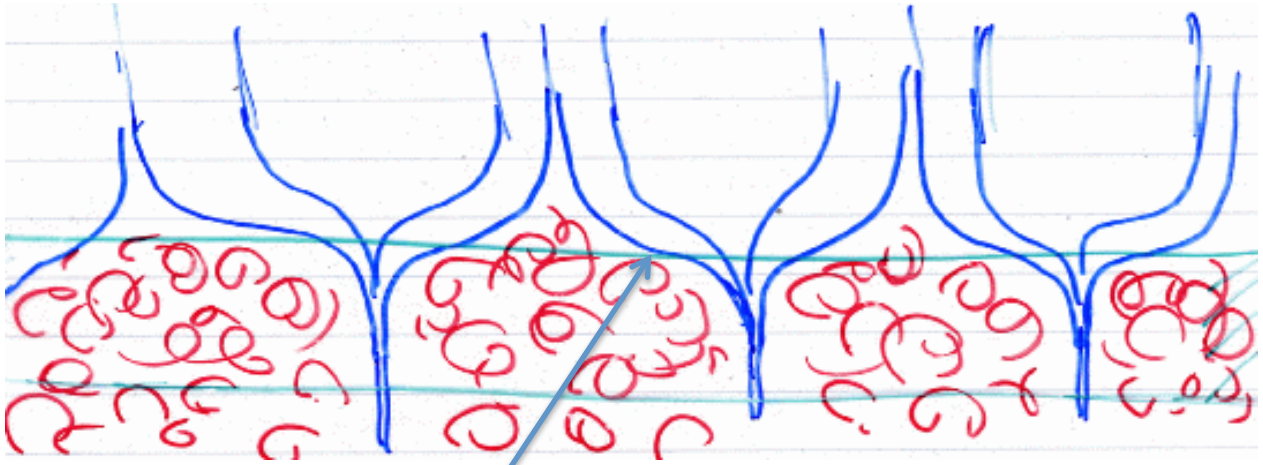

The field becomes more horizontal with height

Anchored loops of various sizes

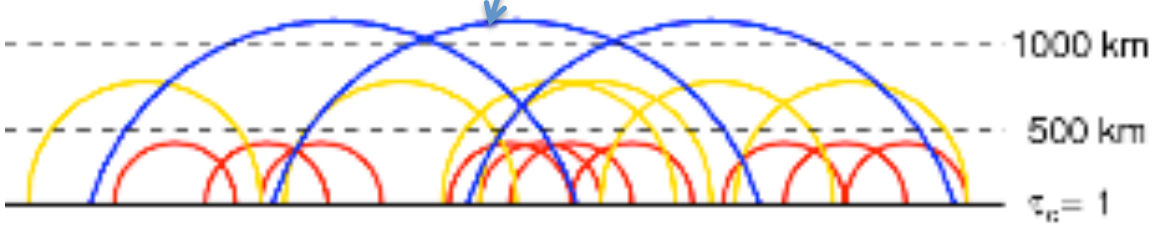

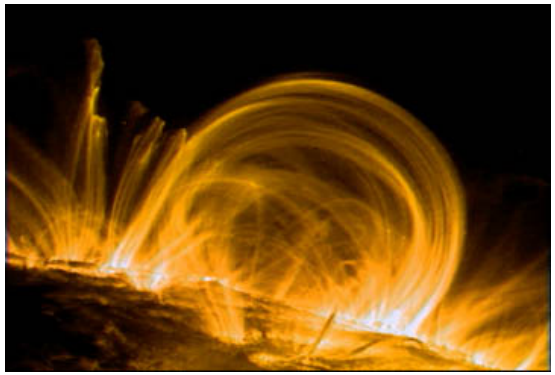

From Steiner 2010

Institute of Astronomy ETH Zurich

Resolution-independent diagnostics

Here we have shown how the properties of the hidden turbulent field and the height variation of the angular distributions can be found in a resolution-independent way. Future telescopes with much higher spatial resolution will not change these results.

The key to the resolution-independence is that our observables are **ensemble averages**, chosen such that optical averaging (when the telescope resolution is low) or numerical averaging over many small resolved spatial elements give identical results.
These two averaging methods are equivalent because we average over a quantity that is proportional to the number of photons.

In observational solar physics there is always a trade-off between spatial, temporal, and spectral resolution and polarimetric precision.
With resolution-independent diagnostics priority is always given to polarimetric precision combined with high spectral resolution, while spatial and temporal resolutions are secondary.

Institute of
Astronomy
ETH Zurich

Thank you !

Institute of
Astronomy
ETH Zurich